Numerical evaluation of systematics in the experiment for electron electric dipole moment measurement in HfF^+

Alexander Petrov *

Petersburg Nuclear Physics Institute named by B.P. Konstantinov of National Research Center "Kurchatov Institute" (NRC "Kurchatov Institute" - PNPI), 1 Orlova roscha mcr., Gatchina, 188300 Leningrad region, Russia and Saint Petersburg State University, 7/9 Universitetskaya nab., St. Petersburg 199034, Russia

(Received 24 August 2023; accepted 16 November 2023; published 4 December 2023)

The energy shifts of hyperfine structure levels of the ground rotational level of the metastable $^3\Delta_1$ electronic state of $^{180}HfF^+$ ions are calculated in the presence of variable external electric and magnetic fields. The calculations are required for the analysis of systematic effects in the experiment for the search of the electron electric dipole moment (*e*EDM). Different perturbations in the molecular spectra important for *e*EDM spectroscopy are taken into account.

DOI: 10.1103/PhysRevA.108.062804

I. INTRODUCTION

Measurement of the electron electric dipole moment (*e*EDM) serves as a highly sensitive probe to test the boundaries of the standard model of electroweak interactions and its extensions [1–3]. The current constrain for *e*EDM $|d_e| < 4.1 \times 10^{-30}$ e cm (90% confidence) was obtained using trapped $^{180}Hf^{19}F^+$ ions [4] with a spinless ^{180}Hf isotope. The measurements were performed on the ground rotational, $J = 1$, level in the metastable electronic $^3\Delta_1$ state. As a matter of fact, the *e*EDM measurement is a highly accurate spectroscopy of $J = 1$ level in the presence of the rotating electric and magnetic fields. It is clear that the accurate evaluation of systematic effects becomes very important with an increase in the statistical sensitivity. The main part of a great success achieved in the solution of this problem in HfF^+ experiment is due to the existence of close levels, the so-called Ω doublets, of the opposite parities. In Ref. [5], possible systematic shifts in the experiment were considered in detail and the corresponding analytical formulas were obtained. In turn, in Refs. [6,7], the theoretical method for the numerical calculation of $J = 1$ hyperfine energy levels in rotating fields was developed. The method demonstrated a very high accuracy in comparison with the latest experimental data [8]. The goal of the present work is to study numerically the selected systematics, taking into account different perturbations in molecular spectra.

The *e*EDM sensitive levels of $^{180}Hf^{19}F^+$ are described in detail in Refs. [5,9,10]. ^{180}Hf isotope is spinless, ^{19}F isotope has a nonzero nuclear spin I=1/2. A hyperfine energy splitting between the levels with the total momentum $F = 3/2$ and $F = 1/2$, $\mathbf{F} = \mathbf{J} + \mathbf{I}$, is several tens of megahertz. In the absence of external fields, each hyperfine level has two parity eigenstates known as the Ω doublets. In the external *static* electric field the $F = 3/2$ states form two (with an absolute value of the projection of the total momentum on the direction of the electric field m_F equal to one half and three halves) Stark doublets levels. Below the levels of the Stark doublet with $|m_F| = 3/2$ will be called upper and lower in accordance to their energies. The upper and lower levels in the doublet are double degenerate. Namely, two Zeeman sublevels connected by the time reversal $m_F \to -m_F$ have the same energy. The levels $m_F = \pm 3/2$ are of interest for the *e*EDM search experiment. The corresponding energy scheme is depicted in Fig. 1 of Ref. [8].

The picture above is for the static electric field. Now let us take into account the fact that the fields in the experiment are the rotating ones. The rotation of electric field causes the degenerate sublevels $m_F = +3/2$ and $m_F = -3/2$ to interact [9]. Therefore, in the case of the *rotating* electric field, the eigenstates have slightly different energies (with the difference denoted by Δ below) and present equal-mixed combinations of $m_F = \pm 3/2$ sublevels which are insensitive to *e*EDM. Note that in the case of the rotating electric field m_F is a projection on the axis (coinciding with the rotating electric field) rotating in the space. In turn, the rotating magnetic field which is parallel or antiparallel to the rotating electric field gives the opposite energy shift for $m_F = +3/2$ and $m_F = -3/2$, and for a sufficiently large magnetic field m_F becomes a good quantum number (as in the static fields) and the corresponding eigenstates again become sensitive to the *e*EDM. We see that the magnetic field, in contrast to the experiments in static fields, is not an (not only an) auxiliary tool but should ensure a nonzero energy shift due to the possible nonzero value of *e*EDM [7,10]. To polarize the molecule completely and to access the maximum *e*EDM signal, both rotating electric and magnetic fields should be large enough, see, e.g., Fig. 2 in Ref. [7]. For these fields, the energy splitting f between $m_F = \pm 3/2$ sublevels is dominated by Zeeman interaction, with a smaller contribution coming from the fact that the rotating fields are used.

The measurement of f is repeated under different conditions which depend on the binary switch parameters such as

*petrov_an@pnpi.nrcki.ru

$\tilde{\mathcal{B}}$, $\tilde{\mathcal{D}}$, $\tilde{\mathcal{R}}$ being switched from $+1$ to -1 (see Refs. [4,10] for details). $\tilde{\mathcal{B}} = +1(-1)$ means that the rotating magnetic field $\mathbf{B}_{\rm rot}$ is parallel (antiparallel) to the rotating electric field $\mathbf{E}_{\rm rot}$; $\tilde{\mathcal{D}} = +1(-1)$ means that the measurement was performed for lower (upper) Stark level; and $\tilde{\mathcal{R}}$ defines the direction for the rotation of the fields around the laboratory z axis: $\vec{\omega}_{\rm rot} = \tilde{\mathcal{R}}\omega_{\rm rot}\hat{z}$, where $\vec{\omega}$ is the angular velocity. The measured f can be expanded as

$$f(\tilde{\mathcal{D}},\tilde{\mathcal{B}},\tilde{\mathcal{R}}) = f^0 + \tilde{\mathcal{D}}f^{\mathcal{D}} + \tilde{\mathcal{B}}f^{\mathcal{B}} + \tilde{\mathcal{R}}f^{\mathcal{R}} + \tilde{\mathcal{B}}\tilde{\mathcal{D}}f^{\mathcal{BD}} + \tilde{\mathcal{D}}\tilde{\mathcal{R}}f^{\mathcal{DR}} + \tilde{\mathcal{B}}\tilde{\mathcal{R}}f^{\mathcal{BR}} + \tilde{\mathcal{D}}\tilde{\mathcal{B}}\tilde{\mathcal{R}}f^{\mathcal{DBR}}, \quad (1)$$

where the notation $f^{S_1,S_2\cdots}$ denotes a component which is odd under the switches $S_1, S_2, \ldots$ and can be calculated by the formula

$$f^{S_1,S_2\cdots} = \frac{1}{8}\sum_{\tilde{\mathcal{B}},\tilde{\mathcal{D}},\tilde{\mathcal{R}}} S_1 S_2 \ldots f(\tilde{\mathcal{D}},\tilde{\mathcal{B}},\tilde{\mathcal{R}}). \quad (2)$$

The eEDM signal manifests as the contribution to the $f^{\mathcal{BD}}$ channel according to

$$\delta f^{\mathcal{BD}} = 2d_e E_{\rm eff}, \quad (3)$$

where $E_{\rm eff}$ is the effective electric field, which can be obtained only in the precise calculations of the electronic structure. The values $E_{\rm eff} = 24$ GV/cm [11,12], 22.5(0.9) GV/cm [13], and 22.7(1.4) GV/cm [14] were obtained. According to Eq. (2)

$$f^{\mathcal{BD}} = \frac{1}{8}\sum_{\tilde{\mathcal{B}},\tilde{\mathcal{D}},\tilde{\mathcal{R}}} \tilde{\mathcal{B}}\tilde{\mathcal{D}} f(\tilde{\mathcal{D}},\tilde{\mathcal{B}},\tilde{\mathcal{R}}). \quad (4)$$

Beyond the eEDM there are a lot of systematics which contribute to $f^{\mathcal{BD}}$ and thus mimic the eEDM signal [5]. The point is that the measurement of other components f^0 (even under all the switches), $f^{\mathcal{D}}$, $f^{\mathcal{B}}$, and others together with their theoretical analysis can tell us about the size of systematic effects and perhaps a way to take them into account [5,8].

II. THEORETICAL METHODS

Following Refs. [6,7,15], the energy levels and wave functions of the ^{180}Hf^{19}F$^+$ ion are obtained by a numerical diagonalization of the molecular Hamiltonian ($\hat{\mathbf{H}}_{\rm mol}$) in the external variable electric $\mathbf{E}$(t) and magnetic $\mathbf{B}$(t) fields over the basis set of the electronic-rotational wave functions

$$\Psi_\Omega \theta^J_{M,\Omega}(\alpha,\beta) U^{\rm F}_{M_I}. \quad (5)$$

Here, Ψ_Ω is the electronic wave function; $\theta^J_{M,\Omega}(\alpha,\beta) = \sqrt{(2J+1)/4\pi} D^J_{M,\Omega}(\alpha,\beta,\gamma=0)$ is the rotational wave function; α, β, γ are Euler angles; $U^F_{M_I}$ is the F nuclear spin wave functions; M (Ω) is the projection of the molecule angular momentum $\mathbf{J}$ on the laboratory $\hat{z}$ (internuclear $\hat{n}$) axis; and $M_I = \pm 1/2$ is the projection of the nuclear angular momentum on the same axis. Note that $M_F = M_I + M$ is not equal to m_F. The latter, as stated above, is the projection of the total momentum on the rotating electric field.

The molecular Hamiltonian for ^{180}Hf^{19}F$^+$ reads

$$\hat{\mathbf{H}}_{\rm mol} = \hat{\mathbf{H}}_{\rm el} + \hat{\mathbf{H}}_{\rm rot} + \hat{\mathbf{H}}_{\rm hfs} + \hat{\mathbf{H}}_{\rm ext}. \quad (6)$$

Here, $\hat{\mathbf{H}}_{\rm el}$ is the electronic Hamiltonian, $\hat{\mathbf{H}}_{\rm rot}$ is the Hamiltonian of the rotation of the molecule, $\hat{\mathbf{H}}_{\rm hfs}$ is the hyperfine interaction between electrons and fluorine nuclei as they are described in Ref. [6], and $\hat{\mathbf{H}}_{\rm ext}$ describes the interaction of the molecule with variable magnetic and electric fields as it is described in Ref. [7].

Depending on the particular form of the time dependence, the interaction with the fields is taken into account within two approaches. In the first one the transition to the rotating frame is performed, whereas in the second approach the quantization of the rotating electromagnetic field is performed. In this paper, the static and time-dependent electric and magnetic fields lie in the xy plane. In this case only rotating with the same frequency electric and magnetic fields are allowed in the first scheme, whereas the second approach is valid for the arbitrary static, rotating, and oscillating fields with arbitrary directions and frequencies [7].

Following Ref. [6], we considered $^3\Delta_1$, $^3\Delta_2$, $^3\Pi_{0^+}$, and $^3\Pi_{0^-}$ low-lying electronic basis states. $\hat{\mathbf{H}}_{\rm el}$ is diagonal on the basis set (5). Its eigenvalues are transition energies of these states. They were calculated and measured in Ref. [16]:

$$\begin{aligned} ^3\Delta_1 &: T_e = 976.930\ {\rm cm}^{-1},\\ ^3\Delta_2 &: T_e = 2149.432\ {\rm cm}^{-1},\\ ^3\Pi_{0^-} &: T_e = 10212.623\ {\rm cm}^{-1},\\ ^3\Pi_{0^+} &: T_e = 10401.723\ {\rm cm}^{-1}. \end{aligned} \quad (7)$$

The electronic matrix elements for the calculation of the molecular Hamiltonian were taken from Ref. [6], except for the hyperfine structure constant $A_\parallel = -62.0$ MHz measured in Ref. [10].

Beyond those listed in Eq. (7), there are other electronic states which can interact with $^3\Delta_1$ (eEDM sensitive state). However, $\Omega > 2$ states are not mixed in the leading order due to the selection rule and can be safely ignored. $^3\Pi_{0^-}$ and $^3\Pi_{0^+}$ states in (7) have the same configuration ($\sim 6s^1 5d^1$, where $6s$ and $5d$ are atomic orbitals of Hf) as $^3\Delta_1$ and therefore have the largest contribution among $\Omega = 0^\pm$ states. Moreover, as described in Ref. [6], the matrix elements between $^3\Pi_{0^\pm}$ and $^3\Delta_1$ were modified to fit the experimental value of the Ω doubling, which effectively takes into account the interaction with other $\Omega = 0^\pm$ electronic states. Among $\Omega = 2$ states the $^3\Delta_2$ state from Eq. (7) also has the largest matrix element with $^3\Delta_1$ (as they have the same configuration) and the energy difference is only about a thousand wave numbers; other $\Omega = 2$ states are much further away and interact much more weakly. We believe that the accuracy of the model is determined by the electronic matrix elements between $^3\Delta_1$ and $^3\Delta_2$ rather than the contribution from other electronic states. Finally, on the base of the comparison of numerical calculations (using the same model as in the present paper) and experimental data (see Ref. [8]), we believe that the accuracy of the model is not worse than 5% for a difference between $f^{\mathcal{BD}}$ in our numerical calculations and analytical formulas in Ref. [5], which is the main topic of the paper.

III. RESULTS

A. Nonreversing magnetic field

In the experiment, the rotating magnetic field $\mathbf{B}_{\rm rot}$ is parallel or antiparallel to the rotating electric field $\mathbf{E}_{\rm rot}$. In an ideal

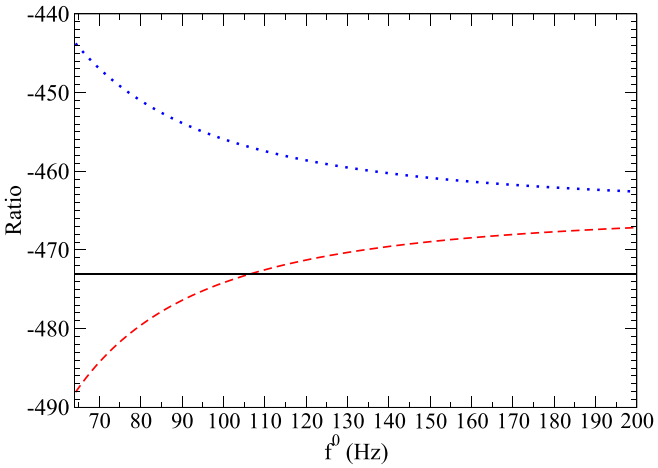

FIG. 1. Calculated ratios $f^{\mathcal{B}}/f^{\mathcal{BD}}$ [dashed (red) curve] and $f^0/f^{\mathcal{D}}$ [dotted (blue) curve] as functions of the component f^0. Also, the constant value $(g^u + g^l)/(g^u - g^l) = -473$ is indicated as a black horizontal line.

case, the absolute value of the magnetic field remains the same after reversing. In the presence of the nonreversing component the absolute values for two directions are different. The nonreversing magnetic field makes an additional contribution to $f^{\mathcal{BD}}$, which leads to the systematic effect, as well as to the $f^{\mathcal{B}}$ component. Both shifts are proportional to the nonreversing component of $\mathbf{B}_{\rm rot}$, and according to Ref. [5], the ratio is

$$\frac{f^{\mathcal{B}}}{f^{\mathcal{BD}}} = \left(\frac{g^u - g^l}{g^u + g^l} - \frac{\Delta^0\Delta^{\mathcal{D}}}{f^{0^2}}\right)^{-1}. \tag{8}$$

Here, g^u and g^l are g-factors of the upper and lower levels of the Stark doublet in the external *static* electric field. Thus, one can remove this systematic monitoring the relatively large $f^{\mathcal{B}}$ component and applying the correction to $f^{\mathcal{BD}}$ on the base of Eq. (8). We note that in the present paper there are no calculations in the static electric field. However, to describe ratios $f^0/f^{\mathcal{D}}$ and $f^{\mathcal{B}}/f^{\mathcal{BD}}$ in the presence of the variable electric field, using the analytical formulas from Ref. [5], g-factors in the static electric field are used. g-Factors in the static electric field were calculated in Ref. [6].

For the numerical calculation of this effect we, according to the first approach mentioned above, perform a transition to the rotating frame. In this case, the rotating fields are replaced by the static ones at the rotating frame:

$$\mathbf{E}(t)_{\rm rot} = \mathcal{E}_{\rm rot}[\hat{x}\cos(\omega_{\rm rot}t) + \hat{y}\sin(\omega_{\rm rot}t)] \to \mathcal{E}_{\rm rot}\hat{X}, \tag{9}$$

$$\mathbf{B}(t)_{\rm rot} = \mathcal{B}_{\rm rot}[\hat{x}\cos(\omega_{\rm rot}t) + \hat{y}\sin(\omega_{\rm rot}t)] \to \mathcal{B}_{\rm rot}\hat{X} \tag{10}$$

and the perturbation

$$\hat{V} = -\vec{\omega}_{\rm rot}\mathbf{F} = -\omega_{\rm rot}\hat{F}_z \tag{11}$$

because the rotation is added to the Hamiltonian. Here x, y, z are the axes of the rotating frame.

The calculated ratio $f^{\mathcal{B}}/f^{\mathcal{BD}}$ as a function of f^0 in Fig. 1 is presented. Also, the calculated ratio $f^0/f^{\mathcal{D}}$ and the calculated value $(g^u + g^l)/(g^u - g^l) = -473$ are given. According to Ref. [5], the ratio is

$$\frac{f^0}{f^{\mathcal{D}}} = \left(\frac{g^u - g^l}{g^u + g^l} + \frac{\Delta^0\Delta^{\mathcal{D}}}{f^{0^2}}\right)^{-1}. \tag{12}$$

In the calculation $\omega_{\rm rot}/2\pi = +375$ kHz and $\mathcal{E}_{\rm rot} = +58$/V/cm, which correspond to the values used in the experiment. To plot Fig. 1, the frequencies f^0, $f^{\mathcal{D}}$, $f^{\mathcal{B}}$, $f^{\mathcal{BD}}$ are assumed to be functions of $\mathcal{B}_{\rm rot}$.

For the values $f^0 = 77$ Hz, 105 Hz, and 151 Hz, used in the experiment [4] (corresponding to $\mathcal{B}_{\rm rot} = 6$, 8, and 12 mG, respectively), we obtain $f^{\mathcal{B}}/f^{\mathcal{BD}} = -481$, -473, and -469, respectively. The latter value corresponds to the solid (black) curve in Fig. 4 of Ref. [8]. The values are not identical to each other and to $(g^u + g^l)/(g^u - g^l)$ due to the rotation perturbation (11). According to Eqs. (8) and (12), the ratios $f^0/f^{\mathcal{D}}$ and $f^{\mathcal{B}}/f^{\mathcal{BD}}$ have a limit $(g^u + g^l)/(g^u - g^l)$. According to our calculations, as Zeeman splitting f^0 increases, the ratios $f^{\mathcal{B}}/f^{\mathcal{BD}}$ and $f^0/f^{\mathcal{D}}$ also approach their saturated value -465, which, however, is different from $(g^u + g^l)/(g^u - g^l) = -473$ on 8. At the same values, the calculated curves $f^0/f^{\mathcal{D}}$ and $f^{\mathcal{B}}/f^{\mathcal{BD}}$ shifted relative to the ones given by Eqs. (8) and (12). We found that the shift is due to the second-order perturbation

$$\frac{\langle m_F = \pm 3/2| - \omega_{\rm rot}\hat{F}_z|m_F = \pm 1/2\rangle^2}{E(m_F = 3/2) - E(m_F = 1/2)} \tag{13}$$

for the energies of the $m_F = \pm 3/2$ states. In this subsection, according to Eq. (9), m_F is the projection of the total momentum on the x axis. If perturbation by the excited $J = 2$ level is taken into account, the numerator in Eq. (13) has a contribution proportional to $\Omega B_{\rm rot}$ (independent of the sign of $m_F = \pm 3/2$). Next, the denominator in Eq. (13) is different by sign and the absolute value for the upper and lower levels of the Stark doublet, which finally leads to the contribution to $f^{\mathcal{B}}/f^{\mathcal{BD}}$ and $f^0/f^{\mathcal{D}}$.

For a given $f^{\mathcal{B}}$, our calculation gives about a 2% larger $f^{\mathcal{BD}}$ value as compared to that given by Eq. (8) from Ref. [5].

B. The second and higher harmonics of $\mathcal{E}_{\rm rot}$

According to the theory of Ref. [5], the additional electric field, oscillating in the xy plane at the double frequency $2\omega_{\rm rot}$ together with the static magnetic field in the same plane, makes additional contributions to $f^{\mathcal{B}}$ but no contribution to $f^{\mathcal{BD}}$, which formally does not lead to a systematic effect. However, applying the correction (8) on the base of the observed $f^{\mathcal{B}}$ does affect the measurement of $f^{\mathcal{BD}}$ component [5].

To calculate this effect, we use variable fields which in addition to the components rotating in the xy plane with the frequency $\omega_{\rm rot}$ [see Eqs. (9) and (10)] consist of the static component of the magnetic field along the laboratory x axis and the electric field with the components along x and y axes which oscillate with frequency $2\omega_{\rm rot}$ and have additional (to rotating component) phase φ:

$$\mathbf{E}(t) = \mathcal{E}_{\rm rot}[\hat{x}\cos(\omega_{\rm rot}t) + \hat{y}\sin(\omega_{\rm rot}t)] + \mathcal{E}_x\hat{x}\cos(2\omega_{\rm rot}t + \varphi) + \mathcal{E}_y\hat{y}\cos(2\omega_{\rm rot}t + \varphi), \tag{14}$$

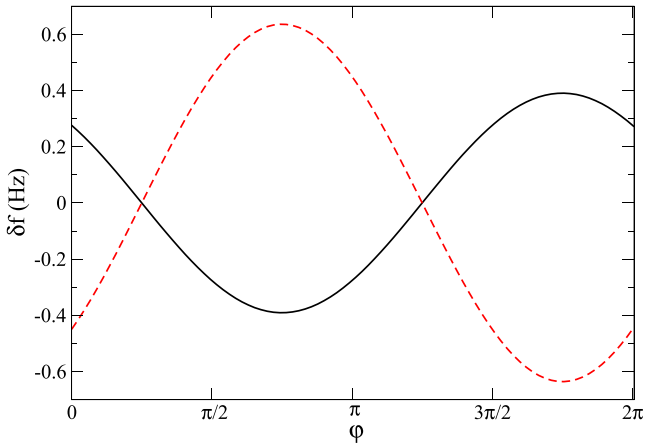

FIG. 2. Calculated $10^4 f^{\mathcal{BD}}$ [solid (black) curve] and $f^{\mathcal{B}}$ [dashed (red) curve] as functions of the phase φ.

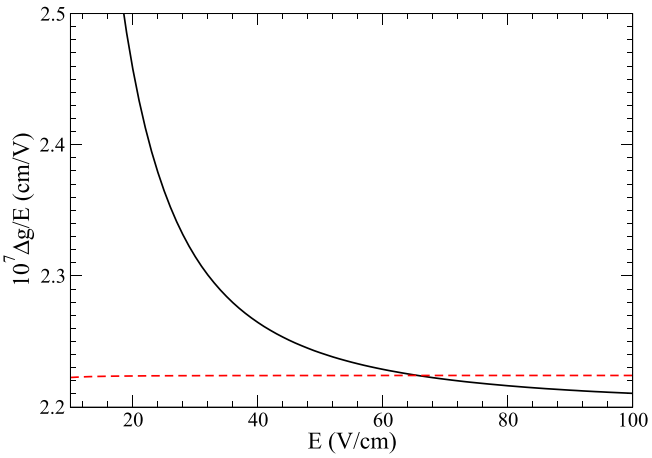

FIG. 3. Calculated $\Delta g/E$ as a function of the external *static* electric field E. Solid (black) curve: magnetic interaction with both $^3\Pi_{0^\pm}$ and $^3\Delta_2$ is taken into account. Dashed (red) curve: the interaction with $^3\Pi_{0^\pm}$ is omitted.

$$\mathbf{B}(t) = B_x\hat{x} + \tag{15}$$

$$\mathcal{B}_{\rm rot}[\hat{x}\cos(\omega_{\rm rot}t) + \hat{y}\sin(\omega_{\rm rot}t)]. \tag{16}$$

Below we put $\omega_{\rm rot}/2\pi = +375$ kHz, $\mathcal{E}_{\rm rot} = +58$ V/cm, $\mathcal{B}_{\rm rot} = \pm 6$ mG (corresponds to $f^0 = 77$ MHz), which are the values used in the experiment [4], and $B_x = 14$ mG and $\mathcal{E}_x = \mathcal{E}_y$, $\mathcal{E}_x/\mathcal{E}_{\rm rot} = 10^{-2}$. Note that $\omega_{\rm rot}$ and $\mathcal{E}_{\rm rot}$ are always positive. In this and following subsections the time dependence of external fields is accounted for by the interaction with the corresponding quantized electromagnetic fields that corresponds to the second approach described in Ref. [7].

In Fig. 2, the calculated values of $f^{\mathcal{BD}}$ and $f^{\mathcal{B}}$ as functions of the phase φ are given. The calculated $f^{\mathcal{B}}$ is in agreement with Fig. 3(b) of Ref. [4]. The general behavior with the presence of the static magnetic field along the y axis is given by Eq. (37) of Ref. [5]. Our calculation also indicates the nonzero value $f^{\mathcal{BD}}$ with the ratio $f^{\mathcal{B}}/f^{\mathcal{BD}} = -1.6 \times 10^4$.

According to the theory of Ref. [5], the nonzero value of $f^{\mathcal{BD}}$ can appear if $\Delta g/E$ depends on the external *static* electric field E. Here, $\Delta g = g^u - g^l$. Figure 3 presents the calculated values of $\Delta g/E$. We present results for the cases when the magnetic interaction with both $^3\Pi_{0^\pm}$ and $^3\Delta_2$ is taken into account and for the case when the interaction with $^3\Pi_{0^\pm}$ is omitted. One can see that if the interaction with $^3\Pi_{0^\pm}$ states is taken into account, the value $\Delta g/E$ depends on the external electric fields. Within a small area of the value of the static electric field, the g-factor difference can be presented as

$$\Delta g = \Delta g_0 + \Delta g_1 E. \tag{17}$$

If the interaction with $^3\Pi_{0^\pm}$ is omitted, $\Delta g_0 = 0$ for a very high accuracy. In Table I, the calculated Δg_0 and Δg_1 for the case when the interaction with $^3\Pi_{0^\pm}$ is taken into account are given. The interaction with $^3\Pi_{0^\pm}$ states ensures nonzero Δg value for the Ω-doublet levels already at the zero external electric field [6]. Note that one of the Ω-doublet states has an admixture of only the $^3\Pi_{0^+}$ state, whereas another one has an admixture of only $^3\Pi_{0^-}$. As the electric field increases, Ω-doublet levels become the Stark-doublet ones with a good Ω quantum number and with an equal admixture of $^3\Pi_{0^+}$ and $^3\Pi_{0^-}$. Therefore, as the electric field increases, the Δg_0 decreases, but is nonzero for any finite electric field. As is stated above, the nonzero Δg_0 leads to nonzero $f^{\mathcal{BD}}$. As the effect is proportional to Δg_0, according to Table I, for $\mathcal{E}_{\rm rot} = 20$ V/cm used in the first stage of the experiment [10] we have $f^{\mathcal{B}}/f^{\mathcal{BD}} = -5.5 \times 10^3$.

Similarly to the second harmonic, the electric field oscillating in the xy plane at the frequency $3\omega_{\rm rot}$ together with the gradient of the magnetic field in the same plane makes additional contributions to both $f^{\mathcal{B}}$ and $f^{\mathcal{BD}}$ with the same (as for the second harmonic) ratio $f^{\mathcal{B}}/f^{\mathcal{BD}} = (g^u + g^l)/\Delta g_0$. The absolute value for $f^{\mathcal{B}}$ is given by Eq. (39) of Ref. [5].

C. Ellipticity of $\mathcal{E}_{\rm rot}$

According to the theory of Ref. [5], the ellipticity of $\mathcal{E}_{\rm rot}$ together with the first-order magnetic field gradient makes additional contributions to $f^{\mathcal{BD}}$ and $f^{\mathcal{B}}$ components with the ratio

$$\frac{f^{\mathcal{B}}}{f^{\mathcal{BD}}} = \frac{3}{4}\frac{g^u + g^l}{g^u - g^l}. \tag{18}$$

TABLE I. The calculated Δg_0 and Δg_1 (cm/V).

E (V/cm)	$10^7\Delta g_0$	$10^7\Delta g_1$
10	19.6	1.27
20	10.1	1.95
30	6.8	2.09
40	5.1	2.14
50	4.1	2.16
60	3.4	2.17
70	2.9	2.18
80	2.6	2.18
90	2.3	2.19
100	2.0	2.19

To calculate this effect we use variable fields

$$\mathbf{E}(\mathrm{t}) = (\mathcal{E}_{\mathrm{rot}} + \mathcal{E}_{\epsilon})\hat{\mathrm{x}}\cos(\omega_{\mathrm{rot}}\mathrm{t}) + (\mathcal{E}_{\mathrm{rot}} - \mathcal{E}_{\epsilon})\hat{\mathrm{y}}\sin(\omega_{\mathrm{rot}}t), \tag{19}$$

$$\mathbf{B}(\mathrm{t}) = \mathcal{B}_{\mathrm{rot}}\frac{\mathcal{E}_{\mathrm{rot}} + \mathcal{E}_{\epsilon}}{\mathcal{E}_{\mathrm{rot}}}\hat{\mathrm{x}}\cos(\omega_{\mathrm{rot}}\mathrm{t}) + \mathcal{B}_{\mathrm{rot}}\frac{\mathcal{E}_{\mathrm{rot}} - \mathcal{E}_{\epsilon}}{\mathcal{E}_{\mathrm{rot}}}\hat{\mathrm{y}}\sin(\omega_{\mathrm{rot}}t) + \mathcal{B}_{\epsilon}\frac{\mathcal{E}_{\mathrm{rot}} + \mathcal{E}_{\epsilon}}{\mathcal{E}_{\mathrm{rot}}}\hat{\mathrm{x}}\cos(\omega_{\mathrm{rot}}t) - \mathcal{B}_{\epsilon}\frac{\mathcal{E}_{\mathrm{rot}} - \mathcal{E}_{\epsilon}}{\mathcal{E}_{\mathrm{rot}}}\hat{\mathrm{y}}\sin(\omega_{\mathrm{rot}}t). \tag{20}$$

In the calculation we put $\mathcal{E}_{\epsilon} = +1$ V/cm, $\mathcal{B}_{\epsilon} = +0.1$ mG. Equation (19) is a rotating electric field, having an ellipticity with a major axis along the x axis. The first two lines of Eq. (20) are a modification of the rotating magnetic field from Eq. (10) caused by the perturbation of the ion micromotion due to the acquired ellipticity of $\mathcal{E}_{\mathrm{rot}}$. This modification actually does not affect the result. The last two lines of Eq. (20) are additional magnetic field feeling by the ion in the first-order magnetic field gradient [5].

The calculation gives $f^{\mathcal{BD}} = -0.913 \times 10^{-4}$ Hz, $f^{\mathcal{B}} = 0.332 \times 10^{-1}$ Hz. The ratio is

$$\frac{f^{\mathcal{B}}}{f^{\mathcal{BD}}} = -364 = 0.757 \times (-481), \tag{21}$$

where -481 (see Sec. III A) is the ratio $f^{\mathcal{B}}/f^{\mathcal{BD}}$ for systematic related to the nonreversing magnetic field for $\mathcal{B}_{\mathrm{rot}} = \pm 6$ mG ($f^0 = 77$ Hz). Note the difference of the coefficient 0.757 in Eq. (21) from the coefficient $3/4 = 0.750$ in Eq. (18). This difference can be explained as follows. Looking at the derivation of Eq. (18) (see Eqs. (43) and (44) in Ref. [5]), one notes that the coefficient 3/4 originates from the fact that $g^u + g^l$ is assumed to be independent of the electric field, whereas $\Delta g = g^u - g^l$ linearly depends on electric field. If $\Delta g = g^u - g^l$ were independent of the electric field, the coefficient in Eq. (18) would be equal to one. We know, however, from the calculation above that Δg has a small fraction (2.7% for $\mathcal{E}_{\mathrm{rot}}$ =58 V/cm as it follows from Table I) which is independent of the electric field. Then, one can calculate that $1 \times 0.027 + 0.750(1 - 0.027) = 0.757$ in accordance to the coefficient in Eq. (21). For the electric field $\mathcal{E}_{\mathrm{rot}}$ =20 V/cm one similarly obtains that the coefficient on the right-hand side of Eq. (21) would be 0.801.

For the given $f^{\mathcal{B}}$, our numerical calculations give about a 1% and 6% smaller $f^{\mathcal{BD}}$ value for the electric fields $\mathcal{E}_{\mathrm{rot}}$ =58 V/cm and $\mathcal{E}_{\mathrm{rot}}$ =20 V/cm, respectively, compared to that given by Eq. (18) from Ref. [5].

IV. CONCLUSION

The accurate numerical calculation of some systematic effects in the experiment for eEDM search on a $^{180}HfF^+$ cation is performed. A small deviation from analytical formulas derived in Ref. [5] is discussed. The results can be used for testing experimental methods and in the next generation of experiments on the HfF^+ cation and on similar systems like ThF^+.

[1] R. Alarcon, J. Alexander, V. Anastassopoulos, T. Aoki, R. Baartman, S. Baeluler, L. Bartoszek, D. H. Beck, F. Bedeschi, R. Berger *et al.*, arXiv:2203.08103 [hep-ph].

[2] Y. Yamaguchi and N. Yamanaka, Phys. Rev. Lett. **125**, 241802 (2020).

[3] Y. Yamaguchi and N. Yamanaka, Phys. Rev. D **103**, 013001 (2021).

[4] T. S. Roussy, L. Caldwell, T. Wright, W. B. Cairncross, Y. Shagam, K. B. Ng, N. Schlossberger, S. Y. Park, A. Wang, J. Ye *et al.*, Science **381**, 46 (2023).

[5] L. Caldwell, T. S. Roussy, T. Wright, W. B. Cairncross, Y. Shagam, K. B. Ng, N. Schlossberger, S. Y. Park, A. Wang, J. Ye *et al.*, Phys. Rev. A **108**, 012804 (2023).

[6] A. N. Petrov, L. V. Skripnikov, and A. V. Titov, Phys. Rev. A **96**, 022508 (2017).

[7] A. N. Petrov, Phys. Rev. A **97**, 052504 (2018).

[8] A. N. Petrov, L. V. Skripnikov, and A. V. Titov, Phys. Rev. A **107**, 062814 (2023).

[9] A. Leanhardt, J. Bohn, H. Loh, P. Maletinsky, E. Meyer, L. Sinclair, R. Stutz, and E. Cornell, J. Mol. Spectrosc. **270**, 1 (2011).

[10] W. B. Cairncross, D. N. Gresh, M. Grau, K. C. Cossel, T. S. Roussy, Y. Ni, Y. Zhou, J. Ye, and E. A. Cornell, Phys. Rev. Lett. **119**, 153001 (2017).

[11] A. N. Petrov, N. S. Mosyagin, T. A. Isaev, and A. V. Titov, Phys. Rev. A **76**, 030501(R) (2007).

[12] A. N. Petrov, N. S. Mosyagin, and A. V. Titov, Phys. Rev. A **79**, 012505 (2009).

[13] L. V. Skripnikov, J. Chem. Phys. **147**, 021101 (2017).

[14] T. Fleig, Phys. Rev. A **96**, 040502(R) (2017).

[15] A. N. Petrov, Phys. Rev. A **83**, 024502 (2011).

[16] K. C. Cossel, D. N. Gresh, L. C. Sinclair, T. Coffey, L. V. Skripnikov, A. N. Petrov, N. S. Mosyagin, A. V. Titov, R. W. Field, E. R. Meyer *et al.*, Chem. Phys. Lett. **546**, 1 (2012).